Dimerization of the scavenger receptor class B type I: formation, function, and localization in diverse cells and tissues

Eve Reaven,[1,*] Yuan Cortez,* Susan Leers-Sucheta,* Ann Nomoto,* and Salman Azhar*,[†]

Geriatrics Research, Education, and Clinical Center,* VA Palo Alto Health Care System, Palo Alto, CA; and Division of Gastroenterology and Hepatology,[†] Department of Medicine, Stanford University School of Medicine, Stanford, CA

Abstract This study has examined the dimeric/oligomeric forms of scavenger receptor class B type I (SR-BI) and its alternatively spliced form, SR-BII, in a diverse group of cells and tissues: i.e., normal and hormonally altered tissues of mice and rats as well as tissues of transgenic animals and genetically altered steroidogenic and nonsteroidogenic cells overexpressing the SR-B proteins. Using both biochemical and morphological techniques, we have seen that these dimeric and higher order oligomeric forms of SR-BI expression are strongly associated with both functional and morphological expression of the selective HDL cholesteryl ester uptake pathway. Rats and mice show some species differences in expression of SR-BII dimeric forms; this difference does not extend to the use of SR-B cDNA types for transfection purposes. In a separate study, cotransfection of HEK293 cells with cMyc and V5 epitope-tagged SR-BI permitted coprecipitation and quantitative coimmunocytochemical measurements at the electron microscope level, suggesting that much of the newly expressed SR-BI protein in stimulated cells dimerizes and that the SR-BI dimers are localized to the cell surface and specifically to microvillar or double membraned intracellular channels. These combined data suggest that SR-BI self-association represents an integral step in the selective cholesteryl ester uptake process.—Reaven, E., Y. Cortez, S. Leers-Sucheta, A. Nomoto, and S. Azhar. **Dimerization of the scavenger receptor class B type I: formation, function, and localization in diverse cells and tissues. *J. Lipid Res.* 2004.** 45: **513–528.**

Supplementary key words selective pathway • cholesterol uptake • high density lipoprotein cholesteryl ester delivery

The "selective" uptake of cholesteryl esters (CEs) from lipoprotein particles, such as HDL, is a process by which the HDL core CE is taken into the cells without the parallel uptake and degradation of the HDL particle itself (1–5). The pathway is a high-capacity, physiologically regulated, bulk cholesterol delivery system (6, 7). Steroidogenic tissues (adrenal gland and gonads) of a variety of animal species, including mouse, hamster, cattle, and human, use this pathway to internalize HDL cholesterol for the production of steroid hormones (6, 7); the pathway is used by the liver to mediate the transfer of cholesterol into bile (6, 7). It operates also in isolated hepatocytes, fibroblasts, adipocytes, and macrophages, although its function in these cell systems is less clear (6, 7).

Scavenger receptor class B type I (SR-BI) is a physiologically relevant receptor identified for the selective pathway (6–11). SR-BI is a member of the class B scavenger receptor family, all members of which contain a large extracellular domain that is anchored to the plasma membrane on each side by transmembrane domains adjacent to short cytoplasmic N- and C-terminal domains (6, 7, 9–11). An alternatively spliced form of SR-BI, termed SR-BII or SR-BI.2, in which 40 entirely different amino acid residues replace 42 of the 45 C-terminal amino acid residues in the C-terminal cytoplasmic domain of SR-BI, has been described in several tissues, including certain cell types in which SR-BI expression is observed (12). The primary function of this protein is not yet known, although it shows significant selective CE uptake function (13).

It is of interest that steroidogenic tissues, which express high levels of SR-BI in vivo, are endowed with an intricate microvillar system for the trapping of lipoproteins. This general region of steroidogenic cells is referred to as the microvillar compartment, and the specialized space created between adjacent microvilli are called microvillar channels (14, 15). It is in the microvillar channels that the various lipoproteins are trapped before the selective uptake of lipoprotein CEs into cells (14–16). Electron microscopic immunocytochemical techniques reveal heavy labeling for SR-BI specifically in these regions (17–19), and

Manuscript received 3 September 2003 and in revised form 5 November 2003.

Published, JLR Papers in Press, December 1, 2003.
DOI 10.1194/jlr.M300370-JLR200

[1] To whom correspondence should be addressed.
e-mail: eve.reaven@med.va.gov

at present, there is no doubt that tissues with microvillar compartments expressing high levels of SR-BI are also active in selective CE uptake.

Indeed, a recent study from this laboratory has shown that the relationship between microvillar channel formation, SR-BI content, and lipoprotein CE uptake in adrenal tissue of rats is hormone-regulated (19). Using hormonal stimulation and withdrawal regimens, we were able to manipulate adrenal SR-BI levels and carry out qualitative and quantitative measurements correlating SR-BI expression with microvillar mass and microvillar channel formation. Young male rats were used as controls, or hormone-stimulated with adrenocorticotropin (ACTH) for 24 h or with 17α-ethinyl estradiol for 5 days, or subjected to a withdrawal of ACTH hormones by dexamethasone treatment (24 h). Quantitative Western blot and immunocytochemistry analyses of adrenals from these animals indicated that ACTH and estradiol treatment greatly increased SR-BI expression (localized especially in the microvillar compartment of adrenocortical cells), whereas dexamethasone treatment led to decreased SR-BI. At the same time, striking ultrastructural changes occurred in the adrenocortical cell microvillar compartment, e.g., microvillar area, microvillar channel length, and microvillar complexity dramatically increased (compared with control values) after ACTH or estradiol treatment, whereas the same measurements showed major declines after dexamethasone treatment. It is of interest that adrenocortical cells of SR-BI knockout mice show microvillar changes similar to those seen in dexamethasone-treated rats (20).

Western blots from these same adrenals also showed a striking difference in the expression of dimeric/oligomeric forms of SR-BI depending on hormonal treatment. (For simplicity, all dimeric and higher order oligomeric forms of SR-BI or SR-BII will be referred to as dimers in this report.) That is, samples of adrenal from animals treated with the stimulatory hormones showed from 2- to 10-fold higher levels of expression of SR-BI dimers/oligomers compared with controls, whereas samples from animals treated with dexamethasone showed far less SR-BI monomer or dimer forms than controls (19). Although Western blot analysis showing SR-BI dimers in adrenal had been observed previously by Landschulz et al. (21), Williams et al. (22), and our group after the use of one or another of these hormonal agents (19), the direct link between SR-BI dimer formation and architectural changes of the microvillar compartment, particularly changes in the extent of channel development, was both surprising and intriguing.

Therefore, in the current study, we sought to characterize the monomeric/dimeric nature of the SR-BI complex in various tissues. Using both biochemical and morphological techniques, we have become convinced that dimeric forms of SR-BI expression are associated with various tissues active in selective CE uptake, and we describe here the dimeric expression of SR-BI (and in some cases its isoform SR-BII) in a diverse group of cells and tissues from normal and hormonally altered tissues of mice and rats as well as in tissues of transgenic animals and transfected cells overexpressing SR-BI.

MATERIALS AND METHODS

Materials

pcDNA6/myc-His, pcDNA6/V5-His, monoclonal anti-V5, and various cell culture media were obtained from Invitrogen Life Technologies (Carlsbad, CA). FUGENE 6 transfection reagent was purchased from Roche Diagnostics Corporation (Indianapolis, IN). The following reagents were supplied by Sigma Chemical Co. (St. Louis, MO): cholesteryl oleate, bovine plasma fibronectin, insulin, transferrin, human chorionic gonadotropin (hCG), Bt_2cAMP, goat anti-rabbit IgG coupled to HRP, anti-cMyc, and galactose oxidase. The LumiGLO Chemiluminescent Substrate System used in Western blotting was obtained from KPL (Gaithersburg, MD). Rabbit anti-mouse IgG coupled to HRP was the product of Zymed (South San Francisco, CA). Goat anti-mouse IgG coupled to 10 nm colloidal gold and goat anti-rabbit IgG coupled to 15 nm colloidal gold were supplied by Ted Pella, Inc. (Reading, CA). All other reagents used were of analytical grade.

Animals and treatment

The Sprague-Dawley male and female rats used in these studies were obtained from Harlan Sprague-Dawley (Indianapolis, IN). Mature (3 month old) rats were treated with a long-acting ACTH gel preparation (10 IU) at 0, 6, 12, and 24 h, or with vehicle alone, and the animals were killed 2 h after the last injection (19). The adrenals were removed, cleaned of adhering fat, and stored at −70°C until analyzed for SR-BI/SR-BII expression. Groups of 3 month old rats (or mice) were treated respectively with 25 IU (or 5 IU) of hCG (or with saline only) every 24 h for 4 days (18). These animals were killed on day 5, and their testes were excised, frozen, and stored at −70°C until analyzed for SR-BI and SR-BII protein expression by Western blotting. For ovary tissue, immature, 22–24 day old rats were injected subcutaneously with 50 IU of pregnant mare's serum gonadotropins (PMSG), followed 56 h later with 25 IU of hCG. Day 0 was considered the day of hCG injection. Such procedures result in superovulated (luteinized) ovaries by day 6 or 7 (17). For desensitized ovaries, the animals were injected with a second dose of hCG (25 IU) between 9:00 and 10:00 AM on day 6 (post-hCG), and ovaries were removed 24 h later (day 7) (17). Control animals received vehicle (saline) only. The freshly isolated ovaries were immediately homogenized and processed for the isolation of "light" and "heavy" membrane fractions using a discontinuous sucrose density gradient technique. For morphological studies, freshly excised adrenal, testes, and luteinized or desensitized ovarian samples were fixed and processed as described previously from this laboratory (17–19).

The SR-BI transgenic mice ($SR\text{-}BI^{Tg}$) used in this study were created in an FVB background and expressed the transgene specifically in the liver at levels ~10-fold higher than those of control FVB mice (23). These mice were kindly provided by Dr. Edward Rubin (Lawrence Berkeley National Laboratory, Berkeley, CA). For other studies, 3 month old male FVB mice were purchased from the Charles River Laboratories (Bloomington, IN).

Isolation and culture of rat granulosa cells

Immature female rats (21–23 days old) were injected subcutaneously with 17β-estradiol (1 mg) daily for 5 days (24, 25). The animals were killed 24 h after their last injection, and granulosa cells were isolated from ovaries and cultured for 72 h in Dulbecco's modified Eagle's medium: F12 medium supplemented with BSA (1 mg/ml), insulin (2 μg/ml), transferrin (5 μg/ml), hydrocortisone (100 ng/ml), and human fibronectin (2 μg/cm^2), as described previously (24, 25). Subsequently, cells were treated with or without Bt_2cAMP (2.5 mM) for an additional 24 h before the addition of other test substances.

Culture conditions for various cell lines

COS-7, CHO, and MLTC-1 cells were cultured in DMEM-10% fetal bovine serum, DMEM-F12-10% fetal bovine serum, and RPMI-1640-10% fetal bovine serum, respectively. R2C and Y1-BS1 cells were cultured in Ham's F10-15% equine serum and 2.5% fetal bovine serum. All media contained penicillin and streptomycin (1%).

Cloning of SR-BI into pcDNA6/c-*Myc*-His and pcDNA6/V5-His vectors

PCR primers against rat SR-BI nucleotide sequence (GenBank accession number D89655) were designed to facilitate the subcloning of full-length rat SR-BI cDNA into the pcDNA6/c-*Myc*-His and pcDNA6/V5-His version B vectors (Invitrogen). The forward primer, 5′-AAGCTTGCGCACGCGAACATGGGC-3′, contained a *Hind*III restriction site and was modified to generate a perfect Kozak sequence for efficient initiation of translation. The reverse primer, 5′-TCTAGACCCAGCTTGGCTTCTTGCAGTAC-3′, contained an *Xba*I restriction site, and the stop codon was mutated to encode a glycine residue to permit the production of SR-BI-c-*myc* or -V5 fusion protein. High-fidelity PCR was conducted using KOD HiFi DNA polymerase (Novagen) and rat SR-BI cDNA (26) as template (6 ng). Two-step PCR cycling consisted of 25 cycles of denaturing and annealing (98°C for 20 s followed by 65°C for 30 s) without extension. The resulting cDNA was subcloned into the pSTBlue-1 vector (Novagen), sequenced on both strands, and then subcloned into the *Hind*III/*Xba*I site of the pcDNA6/c-*myc*-His and pcDNA6/V5-His vectors.

Western blot analysis

The expression of SR-BI and SR-BII proteins in adrenal, liver, testes, ovary tissues, and cultured cells was assessed by Western blot analysis using previously described methodology (17–19, 27). Briefly, intact tissues were homogenized in 10 volumes of buffer (20 mM Tris-HCl, pH 7.5, 2 mM $MgCl_2$, 0.25 M sucrose, 1 mM PMSF, 10 μg/ml leupeptin, 20 μg/ml aprotinin, and 5 μg/ml pepstatin) and centrifuged (800 *g*) for 10 min, and the supernatant was centrifuged for 60 min at 100,000 *g*. The resulting pellet was washed and resuspended in buffer, and the resulting membrane samples were used for immunoblotting of SR-BI and SR-BII. Similarly, cultured cells were washed twice in ice-cold phosphate-buffered saline and lysed in lysis buffer (125 mM Tris-HCl, pH 6.8, 2% SDS, 5% glycerol, 1% 2-mercaptoethanol, 100 mM PMSF, 10 μg/ml leupeptin, 20 μg/ml aprotinin, and 5 μg/ml pepstatin A). After incubation at 37°C for 15 min, each lysate was sonicated briefly to disrupt chromatin (DNA) and then used for immunoblotting.

Aliquots of tissue, cell, or isolated membrane samples were mixed with equal volumes of 2× Laemmli sample buffer [20 mM Tris-HCl, pH 6.8, 2% SDS (w/v), 10% sucrose (w/v), and 1% 2-mercaptoethanol] and subjected to 7% SDS-PAGE. For each sample, a constant amount of protein (2–40 μg) was loaded on the gel. Protein standards (myosin, 200 kDa; β-galactosidase, 116.3 kDa; phosphorylase b, 97.4 kDa; BSA, 66.2 kDa; and ovalbumin, 45 kDa) were also loaded on the gel. After electrophoretic separation, the proteins were transferred to Immobilon polyvinylidene difluoride (PVDF) membranes using standard techniques. The protein blots were incubated with anti-SR-BI or anti-SR-BII for 2 h at room temperature, probed with peroxidase-labeled mouse anti-rabbit IgG, and visualized using the enhanced chemiluminescence (ECL) system. The resulting radiographic chemiluminescence was visualized for different time points (1–10 min), and appropriate films were subjected to densitometric scanning.

Blue native-PAGE for detection of SR-BI dimers and oligomers

Blue native-PAGE (BN-PAGE) was carried out using a slight modification (28) of the procedure of Schägger, Cramer, and von Jagow (29). In brief, aliquots of 100 μg protein samples in 100 μl volume were mixed with 100 μl of buffer containing 40 mM HEPES-KOH, pH 7.0, 2 mM magnesium acetate, and 2% (w/v) digitonin in a final volume of 200 μl. After incubation at 4°C for 30 min, detergent-insoluble material was removed by centrifugation at 20,000 *g* for 20 min at 4°C. One aliquot of the supernatant (80 μl) was mixed with 20 μl of 5× sample buffer [50% glycerol, 25 mg/ml Coomassie blue G-250, 0.375 M 6-amino-*n*-hexanoic acid (6-amino-*n*-caproic acid), and 50 mM Bis-Tris-HCl, pH 7.0] and subjected to PAGE. After electrophoresis, proteins were transferred electrophoretically to a PVDF membrane and subjected to immunoblot analysis as described above (27).

Detection of SR-BI/SR-BI (protein/protein) interactions by coimmunoprecipitation

For coprecipitation studies, HEK293 cells were transiently transfected with 1 μg of SRBI-cMyc-His-pcDNA6 and/or 1 μg of SRBI-V5-His-pcDNA6 constructs (or respective empty vectors) using FUGENE transfection reagent according to the manufacturer's instructions. Forty-eight hours after transfection, cell lysates were prepared. The dishes were washed three times with PBS, lysed with 500 μl of coimmunoprecipitation buffer (20 mM HEPES, pH 7.5, 1 mM EGTA, 1 mM EDTA, 150 mM NaCl, 1% Triton X-100, 1 mM PMSF, and 2.5 μg/ml chymostatin, pepstatin A, leupeptin, and antipain). Lysates were incubated overnight with polyclonal anti-V5 or monoclonal anti-cMyc immune complexes, captured with 50 μl of 50% slurry of protein A/G-agarose beads, and then washed five times with coimmunoprecipitation buffer. Bound proteins were eluted from the beads by boiling and separated by SDS-PAGE. Gels were then immunoprecipitated and immunostained with different combinations of anti-cMyc or anti-V5 primary antibodies [e.g., anti-V5 (for immunoprecipitate) → anti-cMyc (for blot), or anti-cMyc (immunoprecipitate) → anti-V5 (for blot)], and the resulting immunoreactive bands were visualized using an ECL detection system.

Isolation of light and heavy plasma membrane fractions from luteinized and desensitized rat ovaries

Light and heavy plasma membrane fractions were isolated by a slight modification of the procedure described previously (16, 30–32). In brief, pooled ovaries from a group of four superovulated luteinized rats [day 7 post-hCG] or desensitized rats [luteinized ovaries treated with a second (24 h) dose of hCG (25 IU) on day 6] were freed of adhering fat and connective tissue, minced with scissors, and homogenized with 10 strokes in 10 ml of ice-cold STE medium (0.3 M sucrose, 1 M EDTA, and 10 mM Tris-HCl, pH 7.4) at 4°C. After filtration through cheesecloth, the homogenates were subjected to differential centrifugation, and 800 *g* (10 min) and 20,000 *g* (20 min) pellets were prepared and used for the isolation of light and heavy plasma membranes, respectively.

The 800 *g* pellet resuspended in STE medium was layered on the top of a discontinuous sucrose gradient consisting of 5 ml of 30% sucrose, 8 ml of 36% sucrose, 8 ml of 40% sucrose, and 5 ml of 50% sucrose solutions. The gradients were centrifuged at 63,000 *g* for 1 h in a Beckman model L8-70 ultracentrifuge and SW 28 rotor. Unless otherwise stated, the membranes accumulating at the interface between 30% and 36% sucrose were carefully harvested, sedimented, washed, resuspended in STE, and used as a heavy plasma membrane fraction for various studies.

Similarly, to isolate light membranes, the 20,000 *g* pellet was suspended in STE medium and layered on the top of a discontinuous sucrose gradient as described above for heavy membranes. Gradient samples were centrifuged at 63,000 *g* for 4 h using the SW 28 rotor, and the whitish band at the 30–36% interface was

collected, washed, resuspended in STE medium, and used as a light plasma membrane fraction for various studies.

In vitro selective uptake of human HDL_3-derived CEs

Cultured rat ovarian granulosa cells, Y1-BS1 mouse adrenocortical cells, R2C rat Leydig cells, and MLTC-1 mouse Leydig tumor cells were pretreated with Bt_2cAMP (2.5 mM). After 24 h, [^{125}I]dilactitol tyramine-[^{3}H]cholesterol oleolyl ether-human HDL_3 ($hHDL_3$) at 50 μg/ml protein was added to all of the dishes, and the incubations were continued for an additional 5 h. HEK293, COS-7, or CHO cells underwent transient transfection with rat or mouse SR-BI or mouse SR-BII constructs. After 48 h, doubly labeled $hHDL_3$ particles were added, and incubations continued for 5 h. Likewise, Sf9 cells infected for 48 h with recombinant baculovirus coding for rat SR-BI or mouse SR-BII (or infected control cells) were incubated with [^{125}I/^{3}H]$hHDL_3$ particles for 5 h. At the end of the incubation, the cells were washed and then solubilized in 1.2 ml of 0.1 N NaOH. Aliquots (0.5 ml) were precipitated with an equal volume of 20% trichloroacetic acid to determine acid-insoluble and acid-soluble ^{125}I radioactivity or extracted with heptane-isopropanol to determine ^{3}H radioactivity (7, 8).

Under these conditions, trichloroacetic acid-insoluble ^{125}I radioactivity was assumed to represent ^{125}I-labeled protein remaining bound to the cell surface as part of intact lipoprotein (24, 33), and trichloroacetic acid-soluble ^{125}I radioactivity was taken to be internalized, degraded, and accumulated residualizing protein. The uptake of CE was calculated as described earlier (24, 33) and is expressed as nanograms per milligram of cell protein of ^{125}I-labeled (a measure of endocytic uptake) or ^{3}H-labeled (a measure of selective uptake) protein internalized, which, in turn, is determined from the specific activity of the labeled $hHDL_3$ particle (24, 33).

In vivo selective uptake of $hHDL_3$-derived CE

[^{125}I/^{3}H]$hHDL_3$ (150 μg of protein per 100 g of body weight) was administered to rats via the tail vein and circulated in vivo for 90 min (34) before harvesting intact adrenal or ovarian tissues for the determination of ^{125}I and ^{3}H radioactivity and the calculation of rates of selective CE uptake (24, 33). For adrenal studies, 3 month old male rats pretreated with or without ACTH were used; ovarian uptake experiments were conducted using luteinized and desensitized immature rats.

Electron microscope techniques

Single immunostaining technique. Cells or membrane preparations were fixed with 0.05% glutaraldehyde and 4% paraformaldehyde in PBS at pH 7.4 for 2 h, processed, and embedded in LR Gold resin (Ted Pella, Inc.), as previously described (17, 18), but using V5-mAb (6–9 μg/ml) or cMyc-pAb (2–3 μg/ml) in 1% BSA for 2 h at room temperature. The secondary antibody was either goat anti-mouse or anti-rabbit IgG conjugated to 10 nm gold. Gold labeling was done for 1 h at room temperature. The sections were stained with 4% osmium tetroxide, Reynolds' lead citrate, and uranyl acetate before viewing with the electron microscope.

Double immunostaining technique. Cells were fixed and processed as described above. Ultrathin sections on nickel grids were blocked with 3% BSA and then incubated with a mixture of V5-mAb (6–9 μg/ml) and cMyc-pAb (2–3 μg/ml) in 1% BSA for 2 h at room temperature. The secondary antibody was a mixture of goat anti-mouse IgG conjugated to 10 nm gold and goat anti-rabbit IgG conjugated to 15 nm gold. Labeling was done for 1 h at room temperature.

Measurements quantifying membrane area and immunogold labeling of SR-BI. To quantify double membrane concentration in heavy and light membrane preparations from luteinized and desensitized rat ovaries, membrane pellets were processed for immunochemistry, thin sectioned, and stained for SR-BI. Ten random photographs of each immunostained preparation were taken, regions of double membranes were outlined on the photographs, and their areas (as percentage of total area per photograph) were calculated using the Scion-based NIH Image program and Wacom Intuos graphics tablet (Vancouver, WA). Subsequently, the gold particles in the same membrane regions were counted, and gold per 100 mm^2 double membrane areas from both heavy and light membranes were calculated and compared.

Immunogold labeling related to SR-BI dimers. SR-BI dimers were determined morphologically by estimating the distance between two gold particles. At the minimum, each immunogold particle used in immunostaining has attached to it two (100 Å) immunoglobulin (IgG) molecules (one primary plus one secondary antibody), for a total length of ~200 Å, in addition to the SR-BI molecule itself. Thus, if the molecules are entirely stretched out, the distance between any two gold particles would have a maximum length of two such molecules (400 Å) plus whatever small distance [<100 Å, as estimated by fluorescent resonance energy transfer (FRET) techniques (35–37)] lay between the SR-BI molecules forming a dimer. Because the molecules are likely to be folded, this distance will be reduced. We have assumed that taking approximately half this 400 Å length would be reasonable, and we used two times the width of a single cross-sectional slice of plasma membrane (thus, two times the historically accepted value of the 100 Å as the diameter of a plasmalemmal unit membrane) as a visual guide to identify membrane-associated gold "doublets" representing SR-BI dimers. One can make such judgments at any magnification of the photograph because the membrane guide conveniently changes with the magnification.

However, to adjust for the percentage of gold doublets that may represent artifactual clustering of gold, we have used double membrane sites as representative of "specific" staining and nonmembrane sites as representative of "nonspecific" staining, and we adjusted the number of membrane-related gold doublets to reflect this inherent error in the system. As such, the values for SR-BI dimers given in this report may represent an underestimate of actual dimer formation.

Miscellaneous techniques

Apolipoprotein E-free $hHDL_3$ was isolated as described previously. This lipoprotein preparation was used exclusively because the LDL-mediated "endocytic" pathway does not recognize it. For uptake and internalization studies, $hHDL_3$ preparations were conjugated with residualizing labels, i.e., ^{125}I-labeled dilactitol tyramine and [^{3}H]cholesterol oleolyl ether (24, 33). The procedure of Markwell et al. (38) was used to quantify the protein content of $hHDL_3$ and reconstituted HDL preparations. Protein in the cellular lysates was determined as described by Peterson (39).

RESULTS

SR-BI dimer expression in rat adrenal and luteinized ovary

In previous studies, control rat adrenal and luteinized ovary have been used as model tissues demonstrating the in vivo connection between SR-BI expression, microvillar channel formation, and selective HDL-CE selective uptake (14–17). In **Fig. 1**, we see that these tissues express substantial amounts of SR-BI dimers as well.

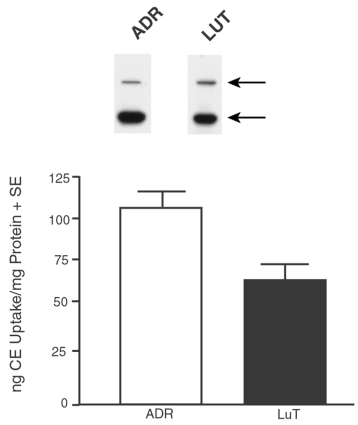

Fig. 1. Representative Western blots showing the presence of scavenger receptor class B type I (SR-BI) dimers in membrane preparations from rat adrenal (ADR) and luteinized ovary (LuT). Membrane fractions from the normal adrenal or luteinized ovary were analyzed by Western blots using SR-BI antibody as described in Materials and Methods. SR-BI exists as a mixture of major monomeric 78–82 kDa bands and minor dimeric 156–164 kDa bands. Molecular weights of monomeric and dimeric forms of SR-BI were calculated from the relative mobility plots of protein standards (myosin, 200 kDa; β-galactosidase, 116.3 kDa; phosphorylase b, 97.4 kDa; BSA, 66.2 kDa; and ovalbumin, 45 kDa). The bar graphs represent selective uptake of human HDL_3 ($hHDL_3$)-derived cholesteryl ester (CE) uptake by these tissues. For these studies, the rats were administered [^{125}I]dilactitol tyramine-[^{3}H]cholesterol oleolyl ether-$hHDL_3$ (150 μg of protein per 100 g of body weight) via tail vein injections. The radioactive mixture was allowed to circulate for 90 min before tissues were excised for the determination of accumulated ^{125}I and ^{3}H radioactivity and the calculation of rates of selective CE uptake. The results shown are means ± SEM from three separate experiments with each tissue. In Western blot, the lower arrow indicates the band for SR-BI monomers, and the upper arrow indicates the band for SR-BI dimers.

Characterization of SR-BI dimers

In this report, a number of control experiments were performed to rule out the possibility that observed SR-BI dimers may be the result of either nonspecific protein aggregation or the formation of nonspecific disulfide linkages during sample preparation. The use of 4 M urea in SDS-PAGE buffer did not alter the SR-BI dimer-monomer ratio in cells or tissues, suggesting that SR-BI dimerization is not the result of nonspecific aggregation of SR-BI protein (data not shown). Likewise, addition of 100 mM iodoacetamide to the homogenization medium (an agent that interacts with sulfhydryl groups on cysteine molecules and prevents the latter from forming disulfide bonds) also failed to prevent the formation of SR-BI dimers (data not shown). Finally, the use of BN-PAGE, which is believed to be less disruptive to protein interactions such as dimer/oligomer formation than the commonly used SDS-PAGE method (40), resulted in information identical to that obtained by the more standard method (data not shown).

SR-BI dimerization and selective CE uptake in diverse SR-BI/SR-BII expressing tissues and cells

In Figs. 2–8, we demonstrate the general relationship between the expression of dimeric forms of SR-BI (and dimeric forms of the SR-BI alternatively spliced isoform, SR-BII) and "selective" CE uptake activity in a diverse group of tissue and/or cell types. In **Fig. 2**, we see the effect of increased trophic hormone stimulation on rat ad-

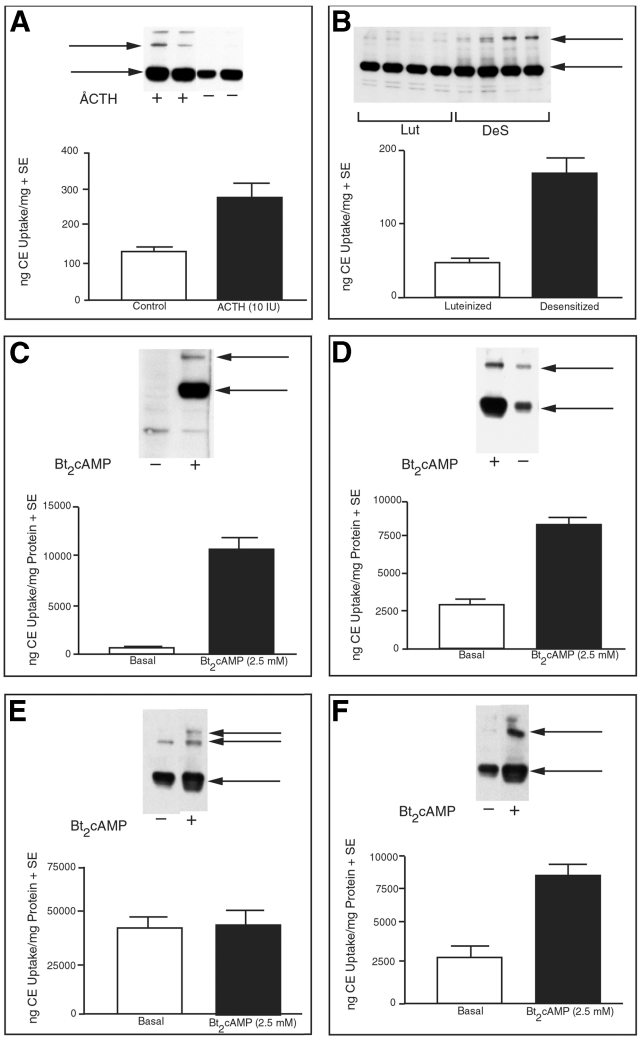

Fig. 2. Expression profiles of SR-BI monomers and dimers and selective CE uptake in diverse hormone-treated steroidogenic cells and tissues. A and B: Sprague-Dawley male rats (A) treated with a long-acting adrenocorticotropin (ACTH) gel or with vehicle alone plus luteinized (LuT) and desensitized (DeS) female rats (B) were injected with [^{125}I/^{3}H]$hHDL_3$ as described for Fig. 1, and rates of selective CE uptake were measured. Aliquots of membrane preparations (10 μg of protein) from these tissues were examined for the presence of SR-BI dimerization by Western blotting. C–F: Cultured ovarian granulosa cells (C), Y1-BS1 adrenocortical cells (D), R2C rat Leydig tumor cells (E), and MLTC-1 mouse Leydig tumor cells (F) were primed with or without Bt_2cAMP (2.5 mM) for 24 h. The cells were then incubated with doubly labeled [^{125}I/^{3}H]$hHDL_3$ for 5 h and processed for the determination of ^{125}I and ^{3}H radioactivity and the calculation of rates of selective uptake. To assess relative levels of expression of SR-BI monomer/dimers, whole-cell lysates were analyzed for immunoreactive SR-BI by Western blotting. The protein concentrations used for ovarian granulosa, Y1-BS1, R2C, and MLTC-1 cells were 20, 40, 4, and 40 μg of protein, respectively. In all panels, the lower arrows shown in Western blots indicate the bands for SR-BI monomers, whereas the upper arrows show SR-BI dimers/oligomers.

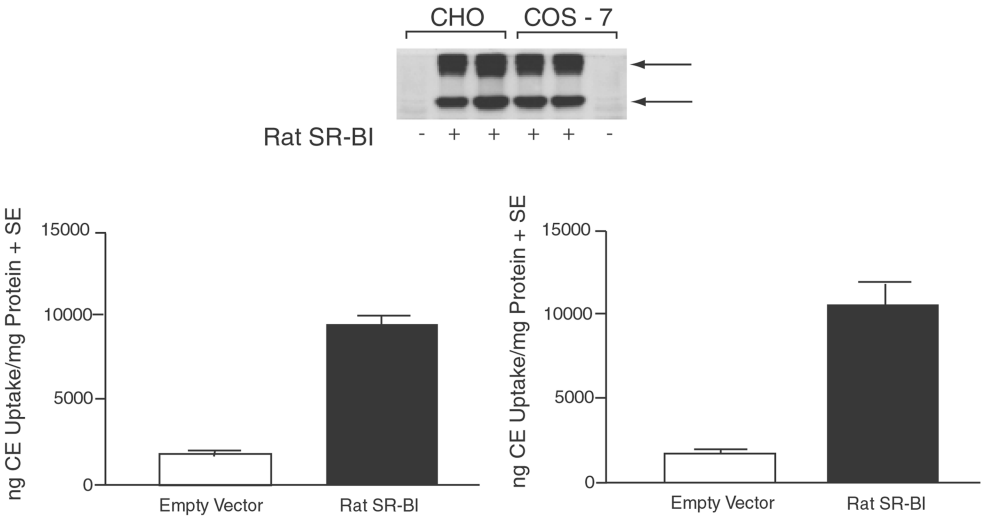

Fig. 3. Expression of SR-BI dimers in CHO and COS-7 cells. Cells were transiently transfected with empty vector or SR-BI-pcDNA6 for 48 h. Whole cell lysates (10 μg protein/lane) were resolved by SDS-PAGE, transferred onto nylon membranes, and probed with anti-SR-BI. Arrows denote the positions of monomeric and dimeric forms of SR-BI and indicate the relatively high dimer-monomer ratio in cells transfected with SR-BI-pcDNA6. Also, rates of selective HDL-CE uptake were three to four times higher in transfected cells than in mock-transfected cells. In Western blot, the lower arrow indicates the band for SR-BI monomers, and the upper arrow indicates the band for SR-BI dimers.

renal and luteinized ovary (Fig. 2A, B), on isolated ovarian granulosa cells growing in vitro (Fig. 2C), and on three different steroidogenic tumor cells lines, Y1-BS1 (Fig. 2D), R2C (Fig. 2E), and MLTC (Fig. 2F). In **Figs. 3** and **4**, we examine genetically altered cells and describe SR-BI monomer and dimer formation and selective CE uptake activity in three nonsteroidogenic cell lines (CHO, COS-7, and HEK293) overexpressing SR-BI. In **Fig. 5**, we look at the situation in a nonmammalian cell (insect Sf9 cells) overexpressing recombinant rat SR-BI and SR-BII, and in **Fig. 6**, the formation of hepatic SR-BI and SR-BII monomers and dimers in SR-BI transgenic mice is shown. Finally, in **Figs. 7** and **8**, we examine differences in SR-BI and SR-BII monomer and dimer formation in two different tissues (adrenal and testis) obtained from different species (mouse and rat). In the adrenal shown in Fig. 7, we see that SR-BI monomer expression in mouse (M) and rat (R) is similar, but far more SR-BI dimers exist in the mouse tissue. With SR-BII, the situation is strikingly different: the mouse adrenal again has high expression of SR-BII monomer (and trace amounts of dimers), whereas the rat adrenal has essentially no SR-BII (either monomer or dimer). With the testis (Fig. 8), the situation is even more complicated. With SR-BI (Fig. 8A), blots show heavier monomer expression of SR-BI in the control rat compared with the control mouse, but monomer plus dimer SR-BI expression is increased in both species by hormone treatment. With SR-BII, the situation is dramatically different (Fig. 8B): basically, the control rat testis expresses only SR-BII dimers, and the control mouse testis expresses only SR-BII monomers. Hormonal stimulation (Fig. 8C) does not change the situation markedly; these hCG-treated rat testes continue to show only SR-BII dimers, and the hCG-treated mouse testis continues to show only SR-BII monomers.

Overall, we find that hormone stimulation in intact cells and tissues, and SR-BI or SR-BII overexpression in various

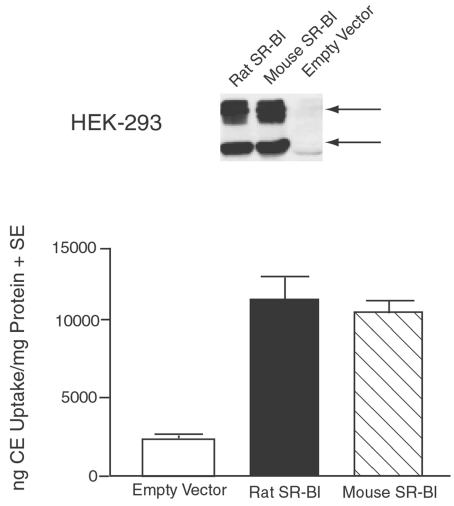

Fig. 4. SR-BI dimer expression and selective uptake in HEK293 cells transfected with rat or mouse SR-BI cDNA constructs. Experimental details were as described for Fig. 3 except that HEK293 cells were transiently transfected with either mouse or rat SR-BI cDNA. Transfection of HEK293 cells with the SR-BI construct resulted in more than a 2-fold increase in the SR-BI dimer/monomer formation, and this effect was independent of the species origin of the construct. A good functional correlation is evident between the increased SR-BI dimer levels and the enhanced (4- to 5-fold) selective HDL-CE uptake. In Western blot, the lower arrow indicates the band for SR-BI monomers, and the upper arrow indicates the band for SR-BI dimers.

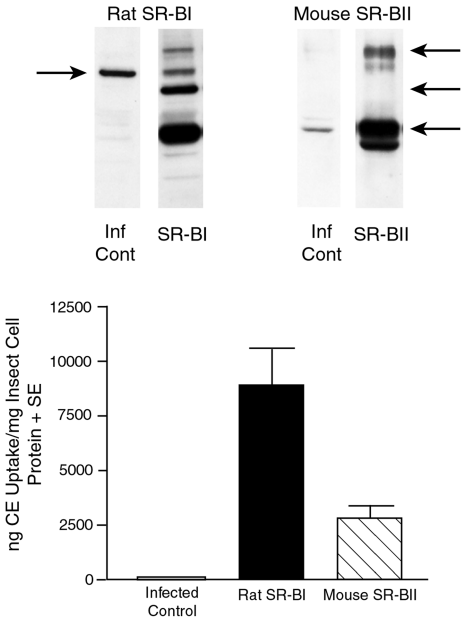

Fig. 5. SR-BI dimer expression and selective HDL-CE uptake in Sf9 insect cells expressing recombinant rat SR-BI or mouse SR-BII. Sf9 cells infected with recombinant baculovirus coding for rat SR-BI, mouse SR-BII, or infected control (Inf Cont) were incubated with doubly labeled [^{125}I/^{3}H]hHDL$_3$ for 5 h and, in each case, the mass of CE internalized via the selective pathway was quantified. In addition, cellular lysates (20 μg of protein) were subjected to SDS-PAGE and Western blotting with anti-SR-BI or anti-SR-BII to measure relative levels of SR-BI/SR-BII monomer and dimeric expression (see arrows). The high dimer expression in SR-BI-infected cells is well correlated with the higher CE uptake in these cells.

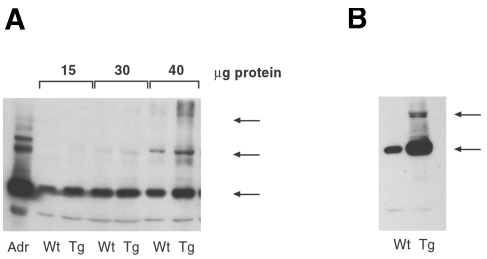

Fig. 6. Western blot analysis of SR-BI and SR-BII dimer expression in hepatic membrane preparations of control [wild type (Wt)] and SR-BI transgenic (Tg) mice. Cell membrane preparations (15–40 μg of protein) from livers of control and SR-BI transgenic mice were subjected to SDS-PAGE, and Western blotting with anti-SR-BI (A) or anti-SR-BII (B) antibodies was performed followed by secondary horseradish peroxidase-conjugated antibodies. The bands were detected by chemiluminescence. The first lane in A represents adrenal (Adr) extract used as a control at a concentration of 15 μg of protein. At every concentration used, higher levels of SR-BI dimers were seen in liver tissue of the SR-BI transgenic mice. Surprisingly high concentrations of hepatic SR-BII monomers and dimers were also formed in the SR-BI transgenic mice. In (A), the lower arrow depicts SR-BI monomers, the middle arrow depicts SR-BI dimers, and the top arrow depicts SR-BI oligomers. In (B), the bottom arrow shows SR-BII monomers and top arrow shows SR-BII dimers.

genetic cell and animal models, always leads to increased dimer formation of the receptor proteins and, whenever measured, increased function of the selective CE uptake pathway. However, tissue and species variations do exist, including unique expression of both SR-BI and SR-BII monomers and dimers (see adrenal and testicular tissues obtained from mice and rats). In evaluating the information in Figs. 2–8, several points should be kept in mind.

a) First, to retain the linear response after treatment (for scanning purposes), it is important that the Western blots not be overexposed; thus, for comparisons of Western blots in the diverse group of cells and tissues studied in Figs. 2–8, one must keep in mind the protein concentrations used for each sample (see legends to individual figures).

b) Except where mentioned, the changes reported are independent of cell type, SR-BI cDNA type (mouse or rat), or reagents used to transfect cell lines. Indeed, despite the use of differing culture conditions for cell lines (dictated by the initial or historical characterization of each cell type), all of the cultured cells studied respond to hormone treatment or SR-BI overexpression by increasing selective CE uptake. The sole exception is the R2C cell, in which similar levels of CE uptake occur before and after Bt_2cAMP stimulation. R2C cells are constitutively programmed to produce large amounts of steroids, and even control levels show unusually high concentrations of both SR-BI monomers and dimers (note that the extract protein concentrations used for Western blots of R2C cells are ~4–10 times less than those used for other steroidogenic cell lines). It is of interest that control R2C cells also constitutively show microvilli and microvillar channels (data not shown) similar to those observed in all steroidogenically active tissues (e.g., adrenal, ovary, testis) (17–19).

c) As seen in **Table 1**, the expression of SR-BI or SR-BII dimers is not simply a function of tissue overproduction of these proteins but rather the effect of trophic hormone action or tissue diversity. Note the nonlinear relationship

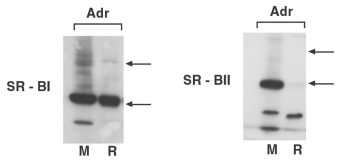

Fig. 7. Relative expression of SR-BI and SR-BII isoforms and dimer formation in adrenals (Adr) of mouse (M) and rat (R). Experimental details for the Western blotting were as described for Fig. 6 except that adrenal membrane preparations of 15 μg of protein were used throughout. Both mouse and rat expressed high levels of SR-BI monomers, but the mouse clearly expressed more SR-BI dimers than the rat at the same protein concentration. Also, SR-BII monomer expression was robust in the mouse adrenal, with barely detectable levels in the rat adrenal. In (A), the lower arrow depicts SR-BI monomers, and the top arrow depicts the area of the gel corresponding to SR-BI dimers. In the mouse gel, the multiple dimer bands probably represent variably glycosylated SR-BI proteins. In (B), the lower arrow represents the position of SR-BII monomers, while the top arrow represents the position of SR-BII dimers.

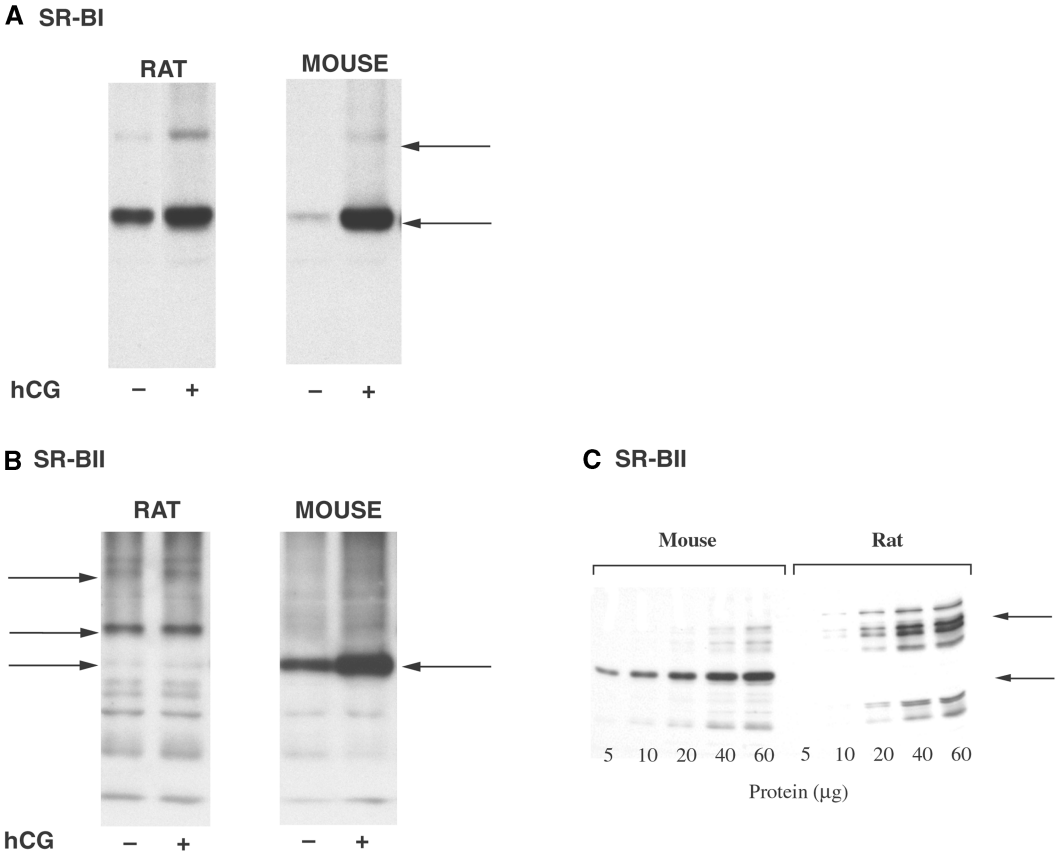

Fig. 8. Gonadotropin regulation of SR-BI and SR-BII expression in rat and mouse testis. Mature (3 month old) rats or mice were treated with 25 IU or 10 IU, respectively, of human chorionic gonadotropin (hCG) every 24 h for 4 days. Total testicular extracts (40 μg of protein) were analyzed for SR-BI and SR-BII expression by Western blotting (see Fig. 6 for details). A: Extracts from control rats displayed more SR-BI monomer/dimer forms than did the mouse extracts. Gonadotropin treatment increased both SR-BI monomers and dimers in extracts from the rat testis and greatly increased mouse monomer forms but not dimer forms of SR-BI. B: Mostly SR-BII dimers are found in the rat testis (with only trace amounts of SR-BII monomers) and only SR-BII monomers are found in the mouse testis (with only trace amounts of SR-BII dimers). C: These SR-BII findings were confirmed when results with various concentrations of protein were analyzed. In all panels, the lower arrows represent SR-BI or SR-BII monomers; the top arrows represent dimer or oligomer forms of these proteins.

between the densitometric measurements of total SR-BI content and the percentage of SR-BI dimer expression in the following: membrane preparations of luteinized versus desensitized ovary; hormone-stimulated versus non-hormone-stimulated rat granulosa, MLTC, and Y1-BS1 cells; and liver expression of SR-BI in wild-type versus SR-BI transgenic mice.

d) Also, SR-BI dimer formation is unlikely to be the function of artifactual protein aggregation during sample processing (e.g., use of urea). Also, iodoacetamide (to minimize the nonspecific formation of disulfide bonds during tissue homogenization) does not alter the relative content of dimers observed in the accompanying Western blots.

e) Sugar-specific lectin affinity chromatography studies indicated that many of the observed SR-BI/SR-BII dimers, especially those obtained from genetically altered cells and tissues, represent heterogeneously glycosylated forms of SR-BI protein (S. Azhar, unpublished observations). As a result, SR-BI dimers often appear in multiple molecular forms on Western blots with small differences in band positions.

SR-BI dimer formation

The experiments described below were used to identify and define newly created SR-BI dimers using biochemical and morphological techniques. The specific strategy used the cotransfection of a cell line (HEK293 cells, which normally express negligible amounts of SRBI/CLA-1) with SR-BI cDNAs containing two different C-terminal tags (SRBI-V5 and SRBI-cMyc) to produce SRBI-V5 and SRBI-cMyc fusion proteins. Specific antibodies to these SRBI-V5 and SRBI-cMyc tags could separately identify the SR-BI fusion proteins produced by the cells.

Coimmunoprecipitation. To directly demonstrate SR-BI dimer formation, HEK293 cells were transfected with either of two SR-BI cDNA constructs epitope-tagged at the C-terminus with c-Myc or V5 sequence. Cell lysates from HEK293

TABLE 1. Quantification of dimer-monomer ratios of SR-BI in various cell/tissue types under different physiological conditions and genetic manipulations

Cells	Dimer/Monomer Ratio	Fold Change[a]
	arbitrary units	
Rat granulosa[b]		
Basal	0	
Bt_2cAMP (2.5 mM)	0.285	ND
Mouse adrenocortical tumor		
Basal	0.087	1.00
Bt_2cAMP (2.5 mM)	0.129	1.48
Mouse Leydig tumor		
Basal	0.030	1.00
Bt_2cAMP	0.301	10.03
Mouse liver		
Control (wild type)	0.170	1.00
SR-BI (transgenic)	0.440	2.59
Heavy membranes from luteinized ovaries	0.039	1.00
Heavy membranes from desensitized ovaries	0.131	3.36

SR-BI, scavenger receptor class B type I.

[a] If SR-BI dimer-monomer relationships were linear, one would expect a constant ratio of 1.00 regardless of the amount of protein made.

[b] No expression of SR-BI is detected in rat granulosa cells cultured under basal (non-hormone-stimulated) conditions.

cells expressing SRBI-cMyc or SRBI-V5 fusion proteins were immunoprecipitated, and Western blots containing the immune complexes were probed with the appropriate antibodies and showed high levels of both SR-BI monomer and dimer formation (**Fig. 9A,** four bands on left side). Cells transfected with empty vector and similarly immunoprecipitated with anti-cMyc or anti-V5 did not express SR-BI proteins (Fig. 9A, center bands). The Western blots presented in Fig. 9A (four bands on right side) confirmed similar high levels of SR-BI epitope-tagged monomer and dimer proteins expressed in cell lysates prepared from preparations cotransfected with the two different epitope-tagged plasmids.

The results shown in Fig. 9B demonstrate that HEK293 cells transfected with one or both types of cDNAs carry out increased selective CE uptake with equal efficiency. In Fig. 9C, we show that the HEK293 cells can be cotransfected with both SR-BI plasmids, precipitated with either anti-cMyc or anti-V5, and immunostained with the alternative antibody (anti-V5 or anti-cMyc). SR-BI proteins are visualized regardless of which antibody was used for immunoprecipitating or immunostaining of the blots. The fact that an immune complex can be precipitated by one antibody and subsequently stained with an antibody to a second protein is consistent with the idea that two proteins are physically associated, presumably in a dimer state.

Coimmunolocalization. A strategy similar to that used for immunoprecipitation was used at the electron microscope level to demonstrate that both forms of the newly produced SR-BI proteins in HEK293 cells are, in fact, translocated in the cell and inserted into appropriate cellular sites. HEK293 cells do not normally have surface microvilli, and the cells express minimal amounts of SR-BI, but long intracellular channels resembling microvillar channels form as a direct result of newly induced SR-BI expression (E. Reaven, unpublished observations). For the most part, these intracellular channels appear to be open to the cell surface (and in occasional cuts one can detect lipoprotein particles trapped in these channels). The cell surface and the new intracellular channels show a robust stain for SR-BI when the specific antibody to SR-BI is used (24). In the current study, we saw that surface and intracellular channel structures similar to those formed by nontagged SR-BI transfection were also formed after transfection of the HEK293 cells with the SR-BI fusion proteins. As seen in **Fig. 10A**, long intracellular channel structures develop in the cells, and these structures can be specifically stained for SR-BI with antibodies to whichever fusion protein was used for transfection (in this case, polyclonal antibody to SRBI-cMyc). Figure 10B shows the specific immunogold staining of the alternative protein, SRBI-V5, in a double membrane ring structure using monoclonal antibody to V5. Given this assurance that the newly formed SR-BI fusion proteins are localized to the same cell surface sites where one normally finds SR-BI, double transfection experiments were carried out in HEK293 cells using both SRBI-V5 and SRBI-cMyc. Sections of the double-transfected cells were simultaneously immunolabeled with a small (10 nm) gold particle (demonstrating monoclonal antibodies to V5) and larger (15 nm) gold particles (demonstrating polyclonal antibodies to cMyc). Such immunostained thin sections viewed with the electron microscope revealed that both forms of the tagged SR-BI could be found on the cell surface and within the newly created intracellular channels (Fig. 10C). Random counts showed that approximately the same number of small gold and large gold particles were in all of these sites. A fair percentage of the gold particles in the channel membranes themselves appeared to be clustered; in one specimen, 6.0% of the total gold particles were doublet forms with two large (15 nm) particles close together, 7% were found as two small (10 nm) gold particles together, and 5% were represented by one small and one large gold particle together. Together, these numbers represent ~18% of the total gold counted. In a second experiment, each of the possible combinations represented nearly equal percentages of the total membrane-associated gold (~7%); together, these numbers represent ~21% of the total gold counted.

These numbers show a more or less even distribution of gold combinations, which would be expected were the doublets to represent SR-BI dimer formation. And overall, the 18–21% of total SR-BI found morphologically as doublets in HEK293 cells is similar to the averaged 26% value obtained by scanning Western blots of the various stimulated tissue samples listed in Table 1.

Localization of SR-BI dimers in membrane preparations

Figures 1 and 2B illustrate the fact that hormone-stimulated rat ovarian tissues express high levels of SR-BI and are able to selectively take in substantial amounts of lipoprotein CEs. In large part, this function is attributable to

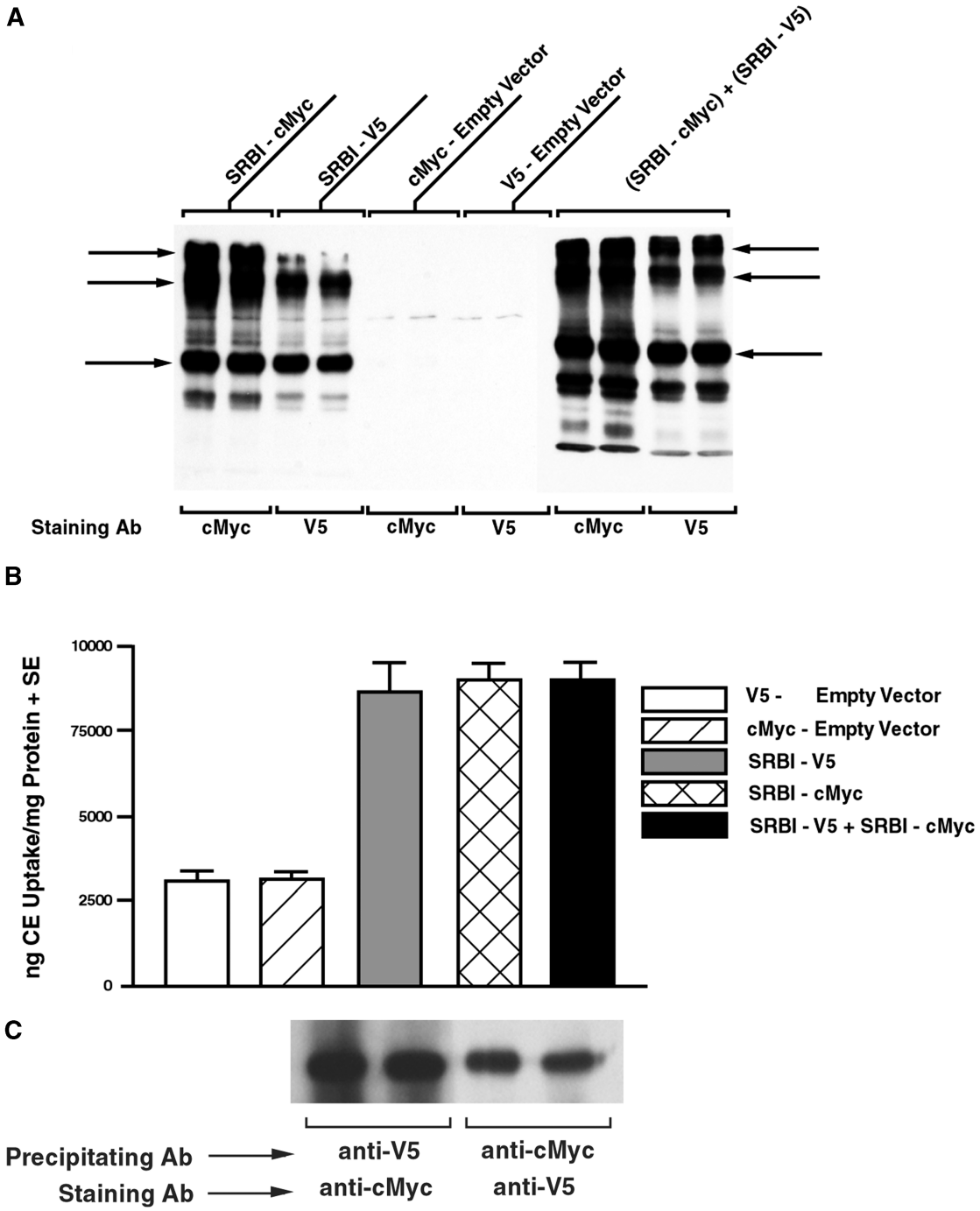

Fig. 9. SR-BI dimer formation in coimmunoprecipitation studies. A: HEK293 cells were transfected with the indicated rat SR-BI constructs SRBI-cMyc (lanes 1 and 2), SRBI-V5 (lanes 3 and 4), empty vectors pcDNA6/V5/His or pcDNA6/c-Myc/His (lanes 5–8), or cotransfected with both SR-BI vectors (lanes 9–12). Cell lysates (20 μg protein/lane) were prepared and subjected to SDS-PAGE and Western blotting using the appropriate antibodies (Ab) to these vectors. The bottom arrow indicates the positions of putative SRBI-cMyc and SRBI-V5 monomers. The top two arrows indicate the presence of SR-BI dimers and oligomers. B: Selective HDL-CE uptake reflects the SR-BI monomer and dimer expression in these transfected cells and indicates no functional variation between the different SR-BI constructs used. C: When cotransfected, the two SR-BI constructs produced different SR-BI proteins, which dimerized with each other. Here, the newly produced tagged SR-BI protein could be precipitated with either anti-V5 (lanes 1 and 2) or anti-cMyc (lanes 3 and 4) antibodies and stained with antibodies to the alternative tag such as anti-cMyc (lanes 1 and 2) or anti-V5 (lanes 3 and 4).

the well-developed surface microvillar compartment inherent in luteinized cells of hormone-treated ovaries (14, 16, 17), a characteristic that permits the isolation of the surface membranes and studies of SR-BI dimer formation. The current studies use highly purified enriched heavy and light plasma membrane preparations from the hormonally responsive rat ovaries, i.e., standard luteinized ovaries from PMSG/hCG-treated rats (high progesterone-

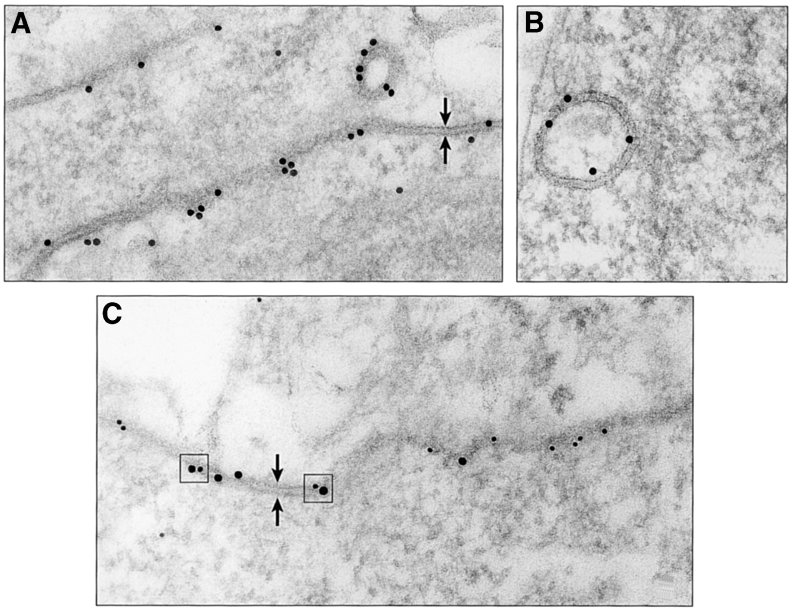

Fig. 10. Electron microscope coimmunolocalization of transfected cMyc and V5 epitope-tagged SR-BI in HEK293 cells. Cells were transfected with either SRBI-cMyc (A) or SRBI-V5 (B), immunostained using polyclonal antibody to the cMyc tag or monoclonal antibody to the V5 tag, and then stained with gold particles associated with the appropriate anti-rabbit or anti-mouse IgG. C: Cells were cotransfected with both SRBI-cMyc and SRBI-V5 and simultaneously immunostained using antibodies to both tags followed by staining with both anti-rabbit and anti-mouse IgG associated with different sized gold particles (i.e., 15 nm anti-rabbit IgG and 10 nm anti-mouse IgG). Arrows indicate the double unit membranes forming the channel wall. The boxed areas in C indicate presumed SR-BI cMyc and V5 dimers, visualized as closely associated gold particles of different sizes. (Note that a minor variation in magnification exists between the three photographs.)

producing tissue that actively obtains cholesterol through the selective CE uptake pathway) and desensitized ovaries from similarly treated animals subjected to 24 h of additional hCG treatment (a tissue that has lost its hormone responsiveness but is very active in recruiting cholesterol through the selective CE uptake pathway) (17). Isolated heavy and light membrane preparations from these hormone-treated animals were also analyzed using the BN-PAGE method and showed monomer-dimer ratios identical to those analyzed with more standard methods.

The heavy membrane fractions from ovaries of both treatments contain large tangled sheets of plasma membranes that, when cut in cross-section, look like unending circular train tracks (**Fig. 11A**). These tracks of plasma membrane double membranes (see high-magnification photograph and drawing in Fig. 11B) represent adjacent microvillar membranes still connected to each other via the external leaflet of each plasma membrane unit (as they are in vivo), with the open space between them representing the microvillar channel space in which exogenously supplied lipoproteins are trapped (14–16). In enriched preparations of such heavy membranes (2, 14, 16, 17), stereological electron microscope measurements indicate that ~25% of the fraction is represented by such double membranes. Note that the regions of this fraction that do not include double membranes show minimal immunogold labeling (Fig. 11A).

In contrast, the light membrane fractions from both luteinized and desensitized ovaries contain only small areas of plasma membrane double membranes; for the most part, these fractions are composed of diverse cytoplasmic constituents, such as mitochondria, patches of vacuolar material, and portions of nuclear material (**Fig. 12A**). Stereological measurements indicate that ~7% of the enriched fractions of light membranes are, in fact, double membranes. Overall, these light membrane fractions contain less SR-BI by Western blot analysis (Fig. 12B) than the heavy membranes, but immunocytochemistry at the electron microscope level followed by stereological measurements show that the amount of SR-BI immunogold labeling corrected for unit area of double membranes within randomly selected photographs is nearly identical in both heavy and light membrane fractions (i.e., on average, there are 5.6 gold particles per 100 mm^2 double membrane in heavy membrane preparations and 5.0 gold particles per 100 mm^2 double membranes in light membrane fractions despite the vast difference in total SR-BI concentration in these fractions) (**Table 2**).

However, Western blots of the four membrane preparations (heavy membranes from luteinized ovaries versus heavy membranes from desensitized ovaries and light membranes from both preparations) show substantial changes in the proportion of SR-BI represented as monomers or dimers (compare Figs. 11C and 12B). Densitometric scanning of the Western blots of the heavy membrane samples from desensitized ovaries indicate that these samples have relatively more dimers (per expressed total SR-BI) than heavy membrane samples from luteinized ovaries (Table 1). And the relative proportion of SR-BI dimers (per expressed total SR-BI) in the heavy membrane fractions is manyfold that of scanned values of the light membrane fractions, in which dimer expression is negligible. It is of interest that when such heavy membrane fractions are immunogold stained for SR-BI (as in Fig. 11A) and viewed with the electron microscope, one finds many gold particles present as doublets, i.e., two gold particles in very close association, as defined in Materials and Methods (Fig. 11B). Indeed, when using the criterion that a distance between two gold particles of less than two times the width of a single plasma membrane represents a gold doublet (potential dimer), we have found that 47–48%, or approximately half of the total 2,100 gold particles counted in 20 photographs of SR-BI-immunostained membrane samples from rat ovaries, were

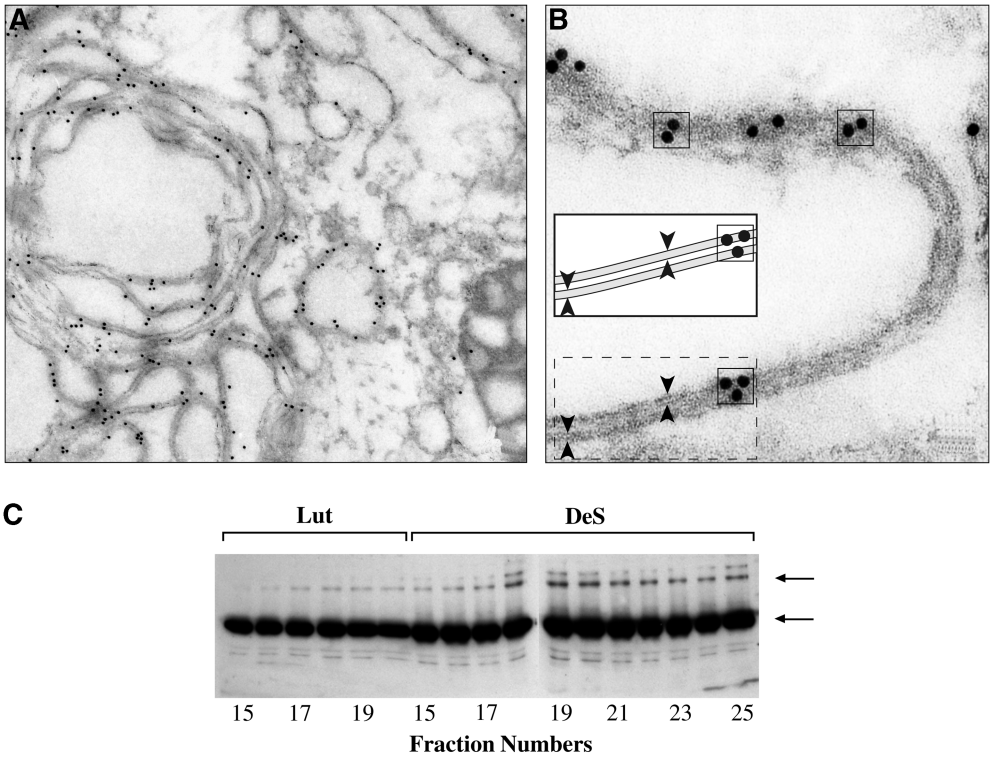

Fig. 11. SR-BI immunocytostaining of SR-BI dimer formation in isolated heavy membrane fractions from luteinized (LuT) and desensitized (DeS) ovaries. A: A typical coil of double (microvillar channel) plasma membranes from the desensitized ovary (fraction 19), which had been immunostained for SR-BI and labeled with 10 nm gold particles. B: One such stained double-membraned channel at high magnification. The arrowheads in B (and in the inset drawing) indicate a region of the channel cut in cross-section and reveal the thickness (~100 Å) of each of the "unit membranes" that line the channel. The boxed gold particles represent particles in very close association with each other, i.e., within a distance no greater than the width of two such unit membranes, or a total of 200 Å (see text). C: The variation in SR-BI dimer/monomer content depending on the tissue model and membrane fraction examined.

found as doublets. No differences were seen in samples from the 10 photographs of heavy membranes from luteinized ovaries and the 10 photographs of membranes from desensitized ovaries (in which 47% versus 48% of total gold was found as doublets). But large differences in the percentage of gold doublets were found between membrane and nonmembrane sites within the same photographs of the membrane preparations, i.e., nonmembrane regions of the same photographs used to view patches of membrane showed that 27% of the total gold found was in the form of doublets. Thus, if one assumes the non-membrane-associated SR-BI gold to indicate nonspecific clustering of the gold and removes that quantity from the calculation, one is left with the possibility that true doublets of SR-BI gold may occur in the membrane sites ~20% of the time.

DISCUSSION

Results from this project strongly suggest that SR-BI exists in dimer and higher order oligomeric forms in cells and tissues that are active in selective uptake of HDL-CEs. In every situation tested (which included such hormone-activated steroidogenic tissues as mouse and rat adrenal, testis, and ovary, steroidogenic-derived cells such as rat ovary luteal cells, mouse adrenal Y1-BS1 cells, rat R2C and MLTC cells, liver from SR-BI transgenic mice, SR-BI transfected nonsteroidogenic cells such as HEK293, Y1BS1, CHO, and COS cells, and primitive Sf9 insect cells programmed to express SR-BI), it is clear that both monomer and oligomeric (defined as dimer) forms of SR-BI are strongly expressed. What is important here is that in the many situations tested, the appearance of SR-BI dimers is associated with both morphological and functional expression of the selective pathway, i.e., the appearance of microvillar channels or intracellular channels that strongly and specifically stain for the SR-BI receptor protein and upregulation of the functional selective pathway shown by increased selective CE uptake from supplied HDL. SR-BI dimers are constitutively expressed in those cells and tissues that are active in selective CE uptake, e.g., mouse and rat adrenal, the rat luteinized ovary, and cells from the rat testis-derived R2C cell line.

Although not tested in every case, the presence and form of SR-BII, the alternative spliced form of SR-BI, appears to show species differences. Whereas SR-BII dimers are plentiful in mouse adrenal, they are not expressed in

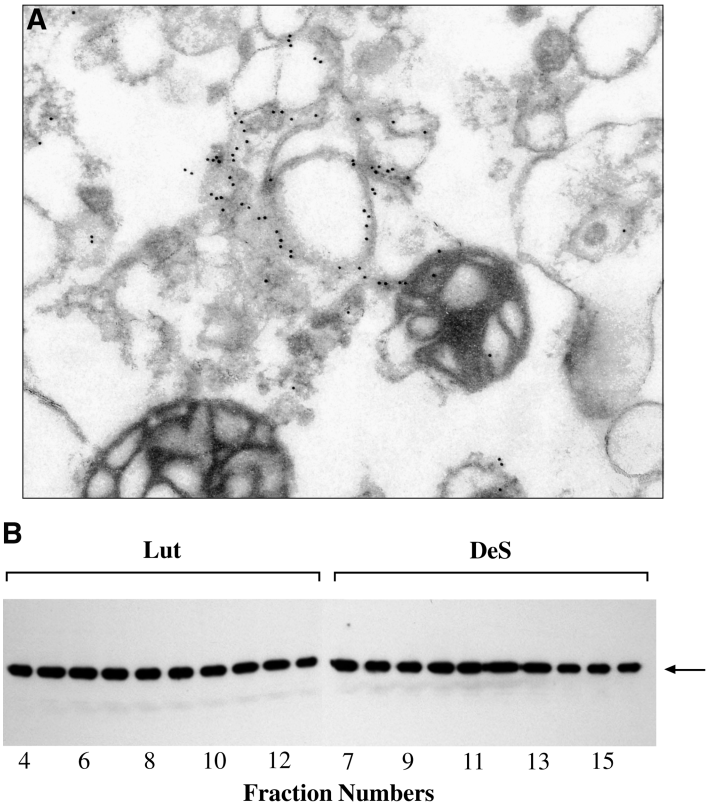

Fig. 12. SR-BI immunocytostaining of SR-BI dimer formation in isolated light membranes from luteinized (LuT) and desensitized (DeS) ovaries. A: A typical image of this fraction with a small area of double membranes expressing SR-BI, as in the heavy membrane fractions shown in Fig. 11, but SR-BI is not found elsewhere in the fraction. B: Only SR-BI monomers are expressed in these light membranes, and the differences in SR-BI expression in luteinized and desensitized ovaries are not seen in light membrane fractions.

rat adrenal, and whereas the mouse testis expresses SR-BII monomers without SR-BII dimers, the rat testis expresses SR-BII dimers without SR-BII monomers. Also, in the SR-BI transgenic mouse liver, there is a large expression of SR-BI, but interestingly, a large number of SR-BII dimers form as well, although no SR-BII dimers are found in livers of the wild-type FVB mice. On the other hand, species differences do not appear to extend to the use of SR-BI cDNAs from either mouse or rat. In the transfection of HEK293 cells with cDNAs of either species, identical expression of both SR-BI and SR-BII isoforms is seen. Although the significance of the SR-BII variations in these tissues is not yet clear, they may signal differences in the way the mouse and rat use these proteins. For example, current morphological studies in our laboratory have shown that rat SR-BII is present in multiple sites of the rat spermatozoa during development, but this is not the situation in mouse spermatozoa (E. Reaven, unpublished observations).

In recent years, one of the most common biochemical approaches used in investigating protein dimerization has been the use of coimmunoprecipitation of differentially epitope-tagged receptors (41–47). In the current project, cotransfection of HEK293 cells with cMyc and V5 epitope-tagged SR-BI was able to show that the newly formed SR-BI proteins had dimerized, i.e., mixtures of two differently tagged proteins permitted both to be precipitated by antibodies to just one of the tags and subsequently visualized on Western blots stained by antibodies to the second tag. This procedure provides direct evidence that SR-BI exists in the transfected HEK293 cells in dimeric forms.

This biochemical evidence of SR-BI dimer formation is positively reinforced by evidence at the electron microscope level that the newly formed SRBI-cMyc or SRBI-V5 has appropriately found its way to the cell surface and resides in the same double-membraned channels where SR-BI is normally found in HEK293 cells after transfection with SR-BI cDNA or, indeed, where SR-BI is found in all steroidogenic cells studied to date (17–19). Moreover, when the two labeled SR-BI proteins are coexpressed and the different proteins are subsequently immunostained and identified with specific sized gold particles, one sees mixing and clustering of the particles, suggesting that not only have the proteins traveled to the same cell location but that they are is close physical association, consistent with the idea that substantial SR-BI dimerization has occurred at these sites. When one calculates the size of the immunoglobulins bound to the commercially available gold particles and estimates the number and size of the at-

TABLE 2. Ovary membrane-associated SR-BI immunogold particles per unit area of double membranes

Sample	Gold Particles/Area (mm^2) of Double Membrane	Gold Particles/100 mm^2 of Double Membrane
Desensitized heavy membranes	2,879/51,408	5.6
Desensitized light membranes	826/16,459	5.0

Regions of double membranes were outlined on photographs, and membrane areas were measured as described in Materials and Methods. Associated gold particles were counted and corrected for unit area (100 mm^2).

tached SR-BI molecules, the physical distance between the clustered gold particles is within the distance accepted for protein dimers by FRET techniques (35–37).

Although there is always some worry about preaggregation of colloidal gold in preparations used for immunostaining, we are confident that this problem is not of major concern in this study. In the case of the cotransfection of the SR-BI fusion proteins in the HEK293 cells, we found three different combinations of gold clusters in approximately equal numbers: one-third are found as doublets of large gold particles, one-third as doublets of small gold particles, and one-third as mixed combinations of small and large gold particles. Such mixed combinations cannot be a result of preaggregated gold. Also, in the portion of the study in which gold clusters in heavy membrane fractions from luteinized and desensitized ovaries were assessed as evidence of SR-BI dimer formation, counts of doublets were compared in specific membrane sites as well as in surrounding sites where some nonspecific staining of structures may occur. If one eliminates the percentage of observed "nonspecific doublets" from the presumed "specific" doublet count, a large number of membrane-related gold doublets still remain unaccounted for. We believe these remaining doublets represent a rough estimate of dimer formation, which, in the case of the strongly labeled heavy membrane fraction of desensitized ovary membranes, represents ~20% of the total gold counted. This figure is commensurate with the estimated 13% of total SR-BI attributed to SR-BI dimers after Western blotting of the heavy membrane fractions.

Although these results demonstrate the prevalence of SR-BI dimers in stimulated tissues that use the selective pathway for cholesterol transport and in large part connect SR-BI dimer formation with SR-BI-enriched channel formation in diverse cells and tissues that use the selective pathway, the role of the SR-BI dimer in these various tissues remains unclear, as it does in many situations in which dimeric protein complexes have been described. Among frequently asked questions is whether dimerized proteins exist as stable preformed dimers or as dynamic monomeric structures that are modulated by ligands (48–54). In the case of SR-BI, one can assume the ligand is HDL or one of several other lipoproteins or lipid-associated molecules (6, 7, 9, 55, 56). We assume that the presence of ligand is not absolutely essential for the formation of SR-BI dimers insofar as both SR-BI monomers and dimers can form in luteal cells maintained in lipid-deficient conditions. Thus, although it is unclear whether SR-BI dimers are preformed or the direct result of ligand binding on the cell surface, conformational changes of the cell surface attributable to hormonal activation or to the activity of secondary factors does appear to be associated with SR-BI dimerization. It is now well established that in the rat adrenal, ovary, and testis that hormonal stimulation (or hormonal removal) can lead to striking architectural changes of the steroid cell surface (17–19) that correlate with dimer formation and altered selective lipoprotein CE uptake. Also, SR-BI formation in nonsteroidal cells as a result of genetic manipulation (HEK293 cells) or baculoviral infection with recombinant DNA (Sf9 cells) appears inevitably to lead to the formation of double-membraned channels. Perhaps in all of these circumstances, the close proximity of two external plasma membrane surfaces containing SR-BI leads to self-association of the SR-BI protein, a mechanism for dimer formation reported in other systems (42–47). The functional consequences of such an event may affect the efficacy of ligand binding and ligand trapping as well as provide scaffolding for cross-talk with a variety of yet unknown secondary factors important to CE trafficking. In this regard, it is of interest that once the double-membraned structures are formed, the connections between the membranes are extremely strong; we know from previous studies that isolating and subjecting adrenal or ovary membranes to sucrose density gradient centrifugation does not break the connections between the channel membranes, and the channels continue to function in trapping lipoproteins in vitro (5) as they do in vivo.

In summary, data from a large and diverse set of cell models indicate that stimulated expression of SR-BI is consistent with the idea of SR-BI self-association and localization to the cell surface, specifically to microvillar channels and/or double-membraned intracellular channels. Although the mechanism by which SR-BI dimerization influences its function is not known, we speculate here that clustering of SR-BI molecules between closely adjacent plasma membrane sites may provide molecular bridges that both maintain the shape of the channel and provide an appropriate conduit for a lipoprotein ligand.

This work was supported by the Office of Research and Development, Medical Research Service, Department of Veterans Affairs, and by Public Health Service Grants HL-33881 and DK-56339 from the National Institutes of Health. The authors are most grateful to Dr. Edward Rubin and Dr. Elaine Gong from the Lawrence Berkeley National Laboratory for supplying tissues from the SR-BI^{Tg} mouse. And the authors thank Mr. Kris Morrow and Mr. Michael Wagner for their special assistance in the preparation of illustrations.

REFERENCES

1. Glass, G., R. C. Pittman, D. B. Weinstein, and D. Steinberg. 1983. Dissociation of tissue uptake of cholesteryl ester from that of apoprotein A-I of rat plasma high density lipoprotein: selective delivery of cholesteryl ester to liver, adrenal, and gonad. *Proc. Natl. Acad. Sci. USA.* **80:** 5435–5439.
2. Reaven, E., Y-D. I. Chen, M. Spicher, and S. Azhar. 1984. Morphological evidence that high density lipoproteins are not internalized by steroid-producing cells during *in situ* organ perfusion. *J. Clin. Invest.* **74:** 1387–1397.
3. Murakami, M., S. Horiuchi, K. Takata, and Y. Morino. 1987. Distinction in the mode of receptor-mediated endocytosis between high density lipoprotein and acetylated high density lipoprotein: evidence for high density lipoprotein receptor-mediated cholesterol transfer. *J. Biochem.* **101:** 729–741.
4. Pittman, R. C., T. P. Knecht, M. S. Rosenbaum, and C. A. Taylor, Jr. 1987. A nonendocytotic mechanism for the selective uptake of high density lipoprotein-associated cholesterol esters. *J. Biol. Chem.* **262:** 2443–2450.
5. Gwynne, G. T., and D. D. Mahaffee. 1989. Rat adrenal uptake and

metabolism of high density lipoprotein cholesteryl ester. *J. Biol. Chem.* **264:** 8141–8150.
6. Azhar, S., and E. Reaven. 2002. Scavenger receptor class BI and selective cholesteryl ester uptake: partners in the regulation of steroidogenesis. *Mol. Cell. Endocrinol.* **195:** 1–26.
7. Azhar, S., S. Leers-Sucheta, and E. Reaven. 2003. Cholesterol uptake in adrenal and gonadal tissues: the SR-BI and 'selective' pathway connection. *Front. Biosci.* **8 (Suppl.):** 998–1029.
8. Acton, S., A. Rigotti, K. T. Landschulz, S. Xu, H. H. Hobbs, and M. Krieger. 1996. Identification of scavenger receptor SR-BI as a high density lipoprotein receptor. *Science.* **271:** 518–520.
9. Krieger, M. 1999. Charting the fate of the "good cholesterol": identification and characterization of the high-density lipoprotein receptor SR-BI. *Annu. Rev. Biochem.* **68:** 523–558.
10. Williams, D. L., M. A. Connelly, R. E. Temel, S. Swarnakar, M. C. Phillips, M. de la Llera-Moya, and G. H. Rothblat. 1999. Scavenger receptor BI and cholesterol trafficking. *Curr. Opin. Lipidol.* **10:** 329–339.
11. Silver, D. L., and A. R. Tall. 2001. The cellular biology of scavenger receptor class B type I. *Curr. Opin. Lipidol.* **12:** 497–504.
12. Webb, N. R., W. J. S. de Villiers, P. M. Connell, F. C. de Beer, and D. R. van der Westhuyzen. 1997. Alternative forms of the scavenger receptor BI (SR-BI). *J. Lipid Res.* **38:** 1490–1495.
13. Webb, N. R., P. M. Connell, G. A. Graf, E. J. Smart, W. J. S. de Villiers, F. C. de Beer, and D. R. van der Westhuyzen. 1998. SR-BII, an isoform of the scavenger receptor BI containing an alternate cytoplasmic tail, mediates lipid transfer between high density lipoproteins and cells. *J. Biol. Chem.* **273:** 15241–15248.
14. Reaven, E., J. Boyles, M. Spicher, and S. Azhar. 1988. Evidence for surface entrapment of cholesterol-rich lipoproteins in luteinized ovary. *Arteriosclerosis.* **8:** 298–309.
15. Reaven, E., M. Spicher, and S. Azhar. 1989. Microvillar channels: a unique plasma membrane compartment for concentrating lipoproteins on the surface of rat adrenal cortical cells. *J. Lipid Res.* **30:** 1551–1560.
16. Reaven, E., X-Y. Shi, and S. Azhar. 1990. Interaction of lipoproteins with isolated ovary plasma membranes. *J. Biol. Chem.* **265:** 19100–19111.
17. Reaven, E., A. Nomoto, S. Leers-Sucheta, R. Temel, D. L. Williams, and S. Azhar. 1998. Expression and microvillar localization of scavenger receptor, class B, type I (a high density lipoprotein receptor) in luteinized and hormone-desensitized rat ovarian models. *Endocrinology.* **139:** 2847–2856.
18. Reaven, E., L. Zhan, A. Nomoto, S. Leers-Sucheta, and S. Azhar. 2000. Expression and microvillar localization of scavenger receptor class B, type I (SR-BI) and selective cholesteryl ester uptake in Leydig cells from rat testis. *J. Lipid Res.* **41:** 343–356.
19. Azhar, S., A. Nomoto, and E. Reaven. 2002. Hormonal regulation of adrenal microvillar channel formation. *J. Lipid Res.* **43:** 861–871.
20. Williams, D. L., J. S. Wong, and R. L. Hamilton. 2002. SR-BI is required for microvillar channel formation and the localization of HDL particles to the surface of adrenocortical cells in vivo. *J. Lipid Res.* **43:** 544–549.
21. Landschulz, K. T., R. K. Pathak, A. Rigotti, M. Krieger, and H. H. Hobbs. 1996. Regulation of scavenger receptor, class B, type I, a high density lipoprotein receptor, in liver and steroidogenic tissues of the rat. *J. Clin. Invest.* **98:** 984–995.
22. Williams, D. L., M. de la Llera-Moya, S. T. Thuahnai, S. Lund-Katz, M. A. Connelly, S. Azhar, G. M. Anantharamaiah, and M. C. Phillips. 2000. Binding and cross-linking studies show that scavenger receptor BI interacts with multiple sites in apolipoprotein A-I and identify the class A amphipathic α-helix as a recognition motif. *J. Biol. Chem.* **275:** 18897–18904.
23. Ueda, Y., L. Royer, E. Gong, J. Zhang, P. N. Cooper, O. Francone, and E. M. Rubin. 1999. Lower plasma levels and accelerated clearance of high density lipoprotein (HDL) and non-HDL cholesterol in scavenger receptor class B type I transgenic mice. *J. Biol. Chem.* **274:** 7165–7171.
24. Azhar, S., L. Tsai, and E. Reaven. 1990. Uptake and utilization of lipoprotein cholesteryl esters by rat granulosa cells. *Biochim. Biophys. Acta.* **1047:** 148–160.
25. Reaven, E., L. Tsai, and S. Azhar. 1996. Intracellular events in the "selective" transport of lipoprotein-derived cholesteryl esters. *J. Biol. Chem.* **271:** 16208–16217.
26. Reaven, E., S. Leers-Sucheta, A. Nomoto, and S. Azhar. 2001. Expression of scavenger receptor class B, type I (SR-BI) promotes microvillar channel formation and selective cholesteryl ester transport in a heterologous reconstitution system. *Proc. Natl. Acad. Sci. USA.* **98:** 1613–1618.
27. Azhar, S., A. Nomoto, S. Leers-Sucheta, and E. Reaven. 1998. Simultaneous induction of an HDL receptor protein (SR-BI) and the selective uptake of HDL-cholesteryl esters in a physiologically relevant steroidogenic cell model. *J. Lipid Res.* **39:** 1616–1628.
28. Yang, T., P. J. Espenshade, M. E. Wright, D. Yabe, Y. Gong, R. Aebersold, J. L. Goldstein, and M. S. Brown. 2002. Crucial step in cholesterol homeostasis: sterols promote binding of SCAP to INSIG-1, a membrane protein that facilitates retention of SREBPs in ER. *Cell.* **110:** 489–500.
29. Schägger, H., W. A. Cramer, and G. von Jagow. 1994. Analysis of molecular masses and oligomeric states of protein complexes by blue native electrophoresis and isolation of membrane protein complexes by two-dimensional native electrophoresis. *Anal. Biochem.* **217:** 220–230.
30. Bramley, T. A., and R. J. Ryan. 1980. Interactions of gonadotropins with corpus luteum membranes. VIII. The different properties of rat luteal cell light and heavy membranes cannot be explained by fractionation of inside-out and outside-out plasma-membrane vesicles. *Mol. Cell. Endocrinol.* **19:** 21–31.
31. Verma, A. K., and J. T. Penniston. 1981. A high affinity Ca^{2+}-stimulated and Mg^{2+}-dependent ATPase in rat corpus luteum plasma membrane fractions. *J. Biol. Chem.* **256:** 1269–1275.
32. Shi, X-Y., S. Azhar, and E. Reaven. 1992. Reconstitution of the lipoprotein cholesteryl ester transfer process using isolated rat ovary plasma membranes. *Biochemistry.* **31:** 3230–3236.
33. Azhar, S., D. Stewart, and E. Reaven. 1989. Utilization of cholesterol-rich lipoproteins by perfused rat adrenals. *J. Lipid Res.* **30:** 1799–1810.
34. Azhar, S., and E. Reaven. 1989. Differences in uptake of high-density lipoproteins by rat adrenals using *in vivo vs. in situ* perfusion techniques. *Biochim. Biophys. Acta.* **1004:** 61–66.
35. Hailey, D. W., T. N. Davis, and E. G. Muller. 2002. Fluorescence resonance energy transfer using color variants of green fluorescent protein. *Methods Enzymol.* **351:** 34–49.
36. Heyduk, T. 2002. Measuring protein conformational changes by FRET/LRET. *Curr. Opin. Biotechnol.* **13:** 292–296.
37. Babu, R., and A. Periasamy. 2003. Fluorescence resonance energy transfer (FRET) microscopy imaging of live cell protein localizations. *J. Cell Biol.* **160:** 629–633.
38. Markwell, M. A. K., S. M. Haas, L. L. Bieber, and N. E. Tolbert. 1978. A modification of the Lowry procedure to simplify protein determination in membrane and lipoprotein samples. *Anal. Biochem.* **87:** 206–210.
39. Peterson, G. L. 1977. A simplification of the protein assay method of Lowry et al. which is more generally applicable. *Anal. Biochem.* **83:** 346–356.
40. Laemmli, U. K. 1970. Cleavage of structural proteins during the assembly of the head of bacteriophage T4. *Nature.* **227:** 680–685.
41. White, J. H., A. Wise, M. J. Main, A. Green, N. J. Fraser, G. H. Disney, A. A. Barnes, P. Emson, S. M. Foord, and F. F. Marshall. 1998. Heterodimerization is required for the formation of a functional $GABA_B$ receptor. *Nature.* **396:** 679–682.
42. Pace, A. J., L. Gama, and G. Breitwieser. 1999. Dimerization of the calcium-sensing receptor occurs within the extracellular domain and is eliminated by Cys → Ser mutation at Cys^{101} and Cys^{236}. *J. Biol. Chem.* **274:** 11629–11634.
43. Byrd, J. C., J. H. Y. Park, B. S. Schaffer, F. Garmroudi, and R. G. MacDonald. 2000. Dimerization of the insulin-like growth factor II/mannose 6-phosphate receptor. *J. Biol. Chem.* **275:** 18647–18656.
44. Gines, S., J. Hillion, M. Torvinen, S. L. Crom, V. Casado, E. I. Canela, S. Rondin, J. Y. Lew, S. Watson, M. Zoli, L. M. Agnati, P. Vernier, C. Lluis, S. Ferre, K. Fuxe, and R. Franco. 2000. Dopamine D1 and adenosine A1 receptors form functionally interacting heteromeric complexes. *Proc. Natl. Acad. Sci. USA.* **97:** 8606–8611.
45. Gomez, I., J. Filipovska, B. A. Jordan, and L. A. Devi. 2002. Oligomerization of opioid receptors. *Methods.* **27:** 358–365.
46. Zhu, C-C., L. B. Cook, and P. M. Hinkle. 2002. Dimerization and phosphorylation of thyrotropin-releasing hormone receptors are modulated by agonist stimulation. *J. Biol. Chem.* **277:** 28228–28237.
47. Saito, Y., J. Haendeler, Y. Hojo, K. Yamamoto, and B. C. Berk. 2001. Receptor heterodimerization: essential mechanism for platelet-derived growth factor-induced epidermal growth factor receptor transactivation. *Mol. Cell. Biol.* **21:** 6387–6394.

48. Lee, S. P., Z. Xie, G. Varghese, T. Nguyen, B. F. O'Dowd, and S. R. George. 2000. Oligomerization of dopamine and serotonin receptors. *Neuropsychopharmacology.* **23 (Suppl.):** 32–40.
49. Latif, R., P. Graves, and T. F. Davies. 2001. Oligomerization of the human thyrotropin receptor: fluorescent protein-tagged hTSHR reveals post-translational complexes. *J. Biol. Chem.* **276:** 45217–45224.
50. Mulcahy, L. 2001. The erythropoietin receptor. *Semin. Oncol.* **28:** 19–23.
51. Rios, C. D., B. A. Jordan, I. Gomes, and L. A. Devi. 2001. G-protein-coupled receptor dimerization: modulation of receptor function. *Pharmacol. Ther.* **92:** 71–87.
52. Angers, S., A. Salahpour, and M. Bouvier. 2002. Dimerization: an emerging concept for G protein-coupled receptor ontogeny and function. *Annu. Rev. Pharmacol. Toxicol.* **42:** 409–435.
53. Schlessinger, J. 2002. Ligand-induced, receptor-mediated dimerization and activation of EGF receptor. *Cell.* **110:** 669–672.
54. Strous, G. J., and J. Gent. 2002. Dimerization, ubiquitylation and endocytosis go together in growth hormone receptor function. *FEBS Lett.* **529:** 102–109.
55. Trigatti, B. F., A. Rigotti, and A. Braun. 2000. Cellular and physiological roles of SR-BI, a lipoprotein receptor which mediates selective lipid uptake. *Biochim. Biophys. Acta.* **1529:** 276–286.
56. Rigotti, A., H. E. Miettinen, and M. Krieger. 2003. The role of the high-density lipoprotein receptor SR-BI in the lipid metabolism of endocrine and other tissues. *Endocr. Rev.* **24:** 357–387.